

Impurity Induced Neutralization of MeV Energy Protons in JET Plasmas

A A Korotkov¹, A Gondhalekar.

JET Joint Undertaking, Abingdon, Oxon, OX14 3EA.

¹ A F Ioffe Institute, St. Petersburg, Russia.

"This document is intended for publication in the open literature. It is made available on the understanding that it may not be further circulated and extracts may not be published prior to publication of the original, without the consent of the Publications Officer, JET Joint Undertaking, Abingdon, Oxon, OX14 3EA, UK".

"Enquiries about Copyright and reproduction should be addressed to the Publications Officer, JET Joint Undertaking, Abingdon, Oxon, OX14 3EA".

ABSTRACT

This paper presents a model elucidating the role of carbon and beryllium, the main impurities in JET plasmas, in neutralizing MeV energy protons. Such protons arise during ion cyclotron resonance frequency (ICRF) heating of deuterium plasmas in the hydrogen minority heating mode D(H), and from D-D fusion reactions. The model establishes charge transfer from hydrogen-like[H] impurity ions to protons as the main process for neutralization. Calculations for deducing the proton energy distribution function $f(E_p)$ from measured hydrogen flux are described. The validity of this model of Impurity Induced Neutralization(IIN) is tested by using it to describe the measured flux in different conditions of plasma heating and fueling. Using this model, and an experimental procedure in which a known change in the density of deuterium atoms at the plasma center is made by applying neutral beam injection(NBI), we have deduced the background thermal deuterium atom density at the plasma center, which is an important new diagnostic result. A full account of the subject of this paper is given in [1].

1. INTRODUCTION: One of the first observations made with the new NPA on JET to measure the distribution of ICRF driven MeV energy protons was that of unexpectedly efficient neutralization of such protons in the plasma center, without recourse to injection of donors for charge-exchange(CX) reactions. We called this "passive" flux. Flux arising when ICRF and NBI were applied together was called "active" flux. The experimental set-up and instrument details are given in [2]. Measurements of "passive" and "active" fluxes are shown in fig.1. Subsequent to [2] the NPA was recalibrated; the corrected data shown here supersedes that in [2]. Before neutralized ICRF driven protons were measured in JET plasma only radiative recombination of protons and electrons, and CX between protons and atoms were considered amongst processes that would cause this flux. The expectation, contrary to fig.1, was of a flux of MeV hydrogen to the NPA arising only upon application of atomic beams to the plasma in the form of NBI from octant 4. Fig.2 shows $\Gamma_H(E)$, energy distributions of the "passive" and "active" hydrogen fluxes.

2. IMPURITY IONS PLAY A KEY ROLE IN NEUTRALIZING MeV PROTONS: From these measurements, we need to account for (i) existence of the "passive" flux, (ii) the "active" flux showing a uniform and energy independent increase over the "passive" when NBI is applied, (iii) in other pulses with D(H) ICRF heating a similar flux, approximately equal to the "active" flux, measured when NBI was applied only at oct.8 on the opposite side of the torus from the NPA. Such observations indicate that the "active" flux is not entirely due to direct CX of protons with NBI atoms at oct.4, and that the main effect of NBI into the plasma is to amplify the process giving rise to the "passive" flux. We show that the flux is, in most part, due to CX between [H] impurity ions and protons. Two key circumstances determine that IIN plays a predominant role in JET plasmas. They are:

2.1. BIG CROSS-SECTIONS FOR CX BETWEEN PROTONS AND [H] IMPURITY IONS: Cross sections for CX between protons and [H] ions of He, Be and C have not been measured. Therefore we have compiled them from best available theoretical calculations. Only CX from ground state of the ions is important for our

considerations. The energy range of interest here, $0.3 \leq E_p (\text{MeV}) \leq 3$, is wide and extends into the high energy Born range ($v \gg Z$). In the vicinity of cross-section maximum ($v \approx Z/\sqrt{2}$) we use results of [3]. In the high energy range ($v > Z$) we employ calculations of [4,5,6]. Our analysis [1] of cross-sections shows that [H] ions of He, Be and C have larger cross-section for CX with protons in the energy range under consideration than background thermal deuterium atoms or beam atoms do. Also the estimated accuracy of cross-sections is enough to accurately determine $f(E_p)$ and the proton tail temperature T_p , for $T_p \leq 0.3 \text{ MeV}$.

2.2. LARGE DENSITY OF IMPURITY DONOR IONS AT THE PLASMA CENTER: At the core of JET plasmas the densities of [H] ions of He, Be and C are comparable to that of beam atoms. We have developed a model for calculating the density of [H] and [He] donors of He, Be and C arising from presence in the plasma of beam (n_b), halo (n_h), background thermal deuterium (n_d) atoms and impurity nuclei (n_z). We compute impurity donor densities using a system of steady-state ion balance equations for bare, [H] and [He] impurity ions. Equation for density of impurity nuclei n_z and of [H] impurity ions n_{z-1} , which are much more abundant than [He] impurity ions, is:

$$I_{z-1} n_{z-1} n_e = n_z \cdot \left\{ 1/\tau_z + \alpha_z n_e + \beta_z n_d + (\langle \sigma v \rangle_{cx_z}^b n_b \gamma_b + \beta_z n_h \gamma_h)_{\text{oct.4}} + (\langle \sigma v \rangle_{cx_z}^b n_b \gamma_b + \beta_z n_h \gamma_h)_{\text{oct.8}} \right\} \quad \text{eq.1}$$

The rate coefficients are: I for ionization of ions by electrons, α for radiative recombination of ions, β for CX of ions with thermal deuterium atoms, $\langle \sigma v \rangle_{cx_z}^b$ for CX between impurity nuclei and beam atoms, and β_z for CX between impurity nuclei and halo atoms. γ_b and γ_h are factors describing coupling of ionization balance between oct.4 and oct.8 during NBI. Except for the unknown n_{z-1} , all parameters in eq.1 are usually well defined. n_z is measured using charge-exchange resonance spectroscopy [7], τ_z is measured variously [8] but here its effect is weak because of observed slow ion transport in the core of JET for most plasma modes. n_d is determined from a comparison of "active" and "passive" hydrogen fluxes. Fig.3 shows deduced densities of the different donors at the center of plasma for the pulse.

2.3. TOTAL PROTON NEUTRALIZATION PROBABILITY: P_ν the total neutralization probability for the protons, is sum of different individual contributions.

$$P_\nu = \langle \sigma v \rangle_{cx_b} \cdot n_b + \langle \sigma v \rangle_{cx_d} \cdot n_d + \langle \sigma v \rangle_{cx_h} \cdot n_h + \sum_q \langle \sigma v \rangle_{cx_q} \cdot n_q + \langle \sigma v \rangle_r \cdot n_e \quad \text{eq.2}$$

$\langle \sigma v \rangle_{cx_{b,d,h,q}}$ are rate coefficients for CX between protons and beam atoms, thermal deuterium atoms, halo atoms, and impurity ions respectively, $\langle \sigma v \rangle_r$ is the radiative recombination rate coefficient. $n_{e,b,d,h,q}$ are densities of electrons, beam atoms, thermal deuterium atoms, halo atoms, and density of [H] and [He] ions of impurities involved, represented by n_q . Fig.4 shows contributions to total P_ν due to different donors present in the plasma.

3. INFERENCE OF ENERGY DISTRIBUTION $f(E_p)$ OF ICRF DRIVEN PROTONS: Then, from the measured fluxes, $f(E_p)$ in the NPA solid angle is inferred thus

$$f(E_1) \cdot P_\nu(E_1) \cdot \gamma(E_1) \cdot S \cdot \Delta E_1 \cdot \mu(E_1) = \{ N(E_1) - N_b(E_1) \} \quad \text{eq.3}$$

Although here $f(E_p)$ is integrated along the line-of-sight the active region has an extent of only $\pm 0.3\text{m}$ about the center [1]. $i=1, \dots, 8$ is the NPA channel number, γ is plasma transparency for the neutralized protons, S is area viewed by the NPA in the observation volume at the plasma mid-plane, ΔE_1 is energy width of each channel, μ is channel detection efficiency, $N(E_1)$ is measured total count rate, and $N_b(E_1)$ is the background noise count rate. Two important applications of the methods discussed in the foregoing are:

3.1. DETERMINATION OF THERMAL DEUTERIUM ATOM DENSITY IN THE PLASMA CORE:

Fig.5 shows comparisons of minority proton energy distribution functions derived from "passive" and "active" fluxes at two close time points where $f(E_p)$ may be assumed constant. Iteration of the value of n_d is performed to obtain a best match of the two distribution functions and thereby the core thermal deuterium density is determined. Varying n_d changes the ratio of $f(E_p)$ derived from the "passive" and "active" fluxes without changing the shape of the distribution function. In fig.5 n_d is varied from $0.5 \times 10^{13} \text{m}^{-3}$ to $2.5 \times 10^{13} \text{m}^{-3}$, the best match is obtained for $n_d = 1.5 \times 10^{13} \text{m}^{-3}$.

3.2. ENERGY DISTRIBUTION AND TAIL TEMPERATURE IN HIGH POWER ICRF HEATING:

An early observation using the new NPA for study of high power ICRF heating was of saturation in energy distribution of measured hydrogen flux [9], and an implied saturation of tail temperature of the ICRF driven protons. Fig.6 shows the inferred ICRF driven $f(E_p)$ at different powers, determined from measured hydrogen flux, and the associated tail temperature T_p . Whereas $\Gamma_H(E)$ showed saturation for $P_{\text{ICRF}} \geq 6\text{MW}$, IIN modeling, using available measured time behaviour of n_z , shows that this comes about due to reduction in impurity concentration during the measurement. In fig.6 $f(E_p)$ evolves as expected up to $P_{\text{ICRF}} = 10\text{MW}$. This emphasizes the importance of impurities and of IIN modeling developed here for interpretation of NPA data.

4. CONCLUSIONS:

1. Impurity Induced Neutralization (IIN) is the dominant neutralization process for MeV energy ICRF driven minority protons in JET plasmas. IIN modeling emphasizes the importance, for interpretation of the high energy NPA flux data, of properly taking into account impurity charge donor densities and the cross-sections for CX with protons.
2. IIN modeling allows inference of effective temperature T_p associated with the proton energy distribution function with good accuracy for $T_p \leq 0.3 \text{ MeV}$. Minority proton density is inferred with $\approx 50\%$ accuracy.
3. A method for determining thermal deuterium density in the core of JET plasmas is developed, based on comparison of "passive" and "active" fluxes. $n_d \approx 10^{13} \text{m}^{-3}$ can be determined with estimated accuracy of $\approx 40\%$.
4. Modeling of ITER plasma predicts that IIN will be a dominant process for neutralization of protons of $E_p \leq 1\text{MeV}$. Using a NPA similar to that used on JET "passive" measurement of ICRF driven protons in ITER will be feasible, without recourse to injection of atomic donors.

5. REFERENCES:

- [1]. A.A.Korotkov and A.Gondhalekar, JET Report, 1994, to be published.
- [2]. M.P.Petrov, et. al., Europhysics Conf. Abstracts, 16C(1992)II-1031.
- [3]. T.G.Winter, Physical Review A35(1987)3799.
- [4]. S.Mukherjee and N.C.Sil, Journal of Physics B13(1980)3421.
- [5]. K.Taulbjerg, R.O.Barrachina and J.H.Macek, Phys. Review A41(1990)207.
- [6]. T.G.Winter and S.G.Alston, Physical Review A45(1992)1562.
- [7]. A.Boileau, et.al., Nuclear Fusion 29(1989)1449.
- [8]. R.Giannella, et.al., Plasma Phys. and Controlled Fusion 34(1992)687.
- [9]. A.A.Khudoleev, et.al., Europhysics Conf. Abstracts, 16E(1992)117.

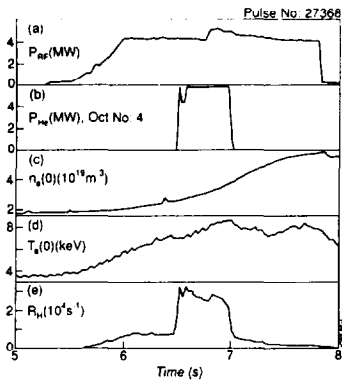


Figure 1

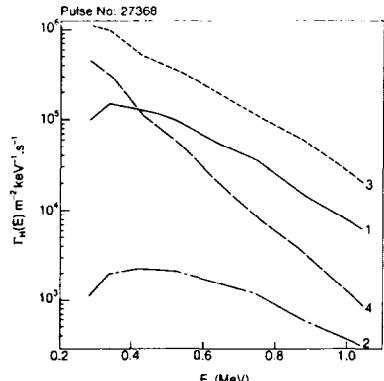


Figure 2

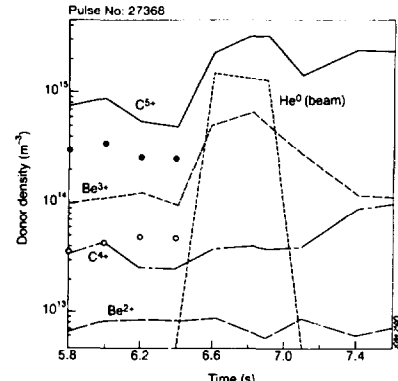


Figure 3

Figure 1-Observation of "passive" and "active" H flux in experiment in which a deuterium plasma with $I_{\phi}=3.5MA$ and $B_{\phi}=2.9T$ was heated with $\approx 6MW$ of NBI power with $120kV$ 4He atoms from oct.4 and $\approx 5MW$ ICRF power for D(H) heating. Traces show evolution of $n_e(0)$, $T_e(0)$, heating powers, and count rate R_H for 0.42 MeV H^0 flux received into the NPA. The "passive" flux arose with application of ICRF power, and independently of NBI. The "active" flux arose only when NBI and ICRF powers were applied together.

Figure 2-Energy distribution of hydrogen flux, $\Gamma_H(E)$, showing spectrum of: (1) measured "passive" flux at $6.4s$, (2) "passive" flux if radiative recombination were its source, (3) measured "active" flux at $6.6s$, (4) "active" flux if direct CX with beam atoms were its source. In [1] we deduce that neither CX with beam atoms, nor recombination with plasma or 'cold' beam electrons, are sufficient to give the observed large flux or its energy dependence.

Figure 3-Comparison of density of donors at the plasma center at oct.4. These consist of He^0 atoms from $5.8MW$ of 120 kV beams, $[H]$ and $[He]$ ions of C and Be deduced using measured impurity nuclear densities and the ion balance model developed here. Impurity nuclear densities at $t=6.6s$, measured using charge-exchange resonance spectroscopy[7], were: $n_{C,Be,He}(m^{-3}) = 10^{18}, 9 \times 10^{17},$ and 2×10^{18} .

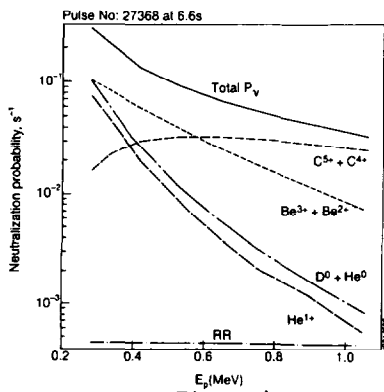


Figure 4

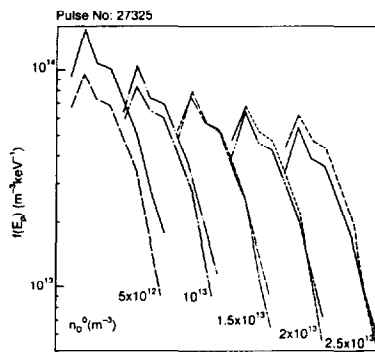


Figure 5

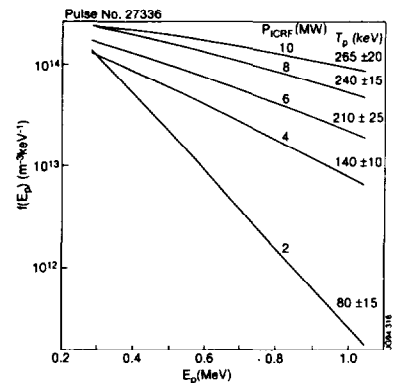


Figure 6

Figure 4- Total neutralization probability for protons is the sum over all donors, $P_V = \sum \langle \sigma v \rangle_{CX} \cdot n_{DO}$, showing contributions due to (1) C^{5+} and C^{4+} , (2) Be^{3+} and Be^{2+} , (3) He^{1+} , and (4) beam of atoms of He^0 from oct.4 and background thermal deuterium atoms D^0 , and (5) radiative recombination of electrons and protons(RR).

Figure 5- Proton energy distribution function inferred from "passive" and "active" fluxes at two close time points where $f(E_p)$ may be assumed constant. n_d was iterated to obtain agreement between $f(E_p)$ derived from the two fluxes. Five iterations of n_d are shown, the best match was obtained for $n_d=1.5 \times 10^{13} m^{-3}$. Constant $\tau_z=2.5$ s was used in the calculations. However, τ_z does not have much effect on the resulting best value of n_d , for $\tau_z \geq 0.5$ s.

Figure 6- Best fitting Stix-like energy distribution function for minority protons driven by ICRF, showing variation of $f(E_p)$ and associated tail temperature T_p with applied power. The experimental proton distribution function was inferred from hydrogen flux measurements described in [9].